Supplementary Information

Topological Polymorphism of the Two-start Chromatin Fiber

Davood Norouzi and Victor B. Zhurkin

A: Calculating optimal geometry of the inter-nucleosomal linkers

Finding conformation of the DNA linker connecting two nucleosomes is the special case of a general polymer chain closure problem. This problem has been solved for the all-atom models of the polypeptide [S1] and nucleic acid [S2] chains previously. Here, because of an extremely large size of the system, we use a 'mesoscopic' approach [S3] where DNA is modeled at the level of dimeric steps, and its trajectory is described by the six base-pair step parameters Twist, Roll, Slide, etc. [S4]. The main idea remains the same, however – one has to join the two chain ends. To build the linker connecting nucleosomes ν1 and ν2, we start at the exit point of ν1 (Fig. 1A) and, for any given set of the DNA parameters, generate positions of the L base pairs of the linker plus one 'virtual' base pair #(L+1). Our goal is to find the values of DNA parameters that bring the base pair #(L+1) at the end of the linker in the same position and direction as the base pair #1 at the entry point of ν2 (Fig. 1A).

To this aim, the penalty function (evaluating the difference between the positions of the two base pairs) is calculated as the sum of squares of the distances between the ends of the reference vectors X, Y and Z for the two base pairs. This penalty is added to the elastic energy of the linker DNA [33] and the net function is minimized using a standard method of numeric minimization (described in detail earlier [S5]). Typically, in the end of minimization the distances between the ends of the two sets of the vectors X, Y and Z are less than 0.05 Å. The DNA linker minimization is nested in an outer cycle in which the total energy of the nucleosome fiber is minimized as a function of the four parameters defining the fiber configuration.

B: Energy terms

(I) DNA Elastic energy. The elastic energy of the linker DNA deformation is calculated using the knowledge-based potential functions introduced by Olson et al. [33]. The stiffness constants, including the cross correlations (such as Twist-Roll) are taken as averages for all 16 dinucleotides. As the rest-state values we use the average helical parameters of B-DNA: Twist = 34.5° and Rise = 3.35 Å (the other rest-state values, such as Slide, are taken to be zero).

(II) Electrostatic energy. The electrostatic energy is calculated using the Coulomb potential with 30 Å distance cutoff and the water dielectric constant ε = 78. (In addition, we made computations with the Debye-Huckel potential; see section D) We assume that it is the DNA surface which is the subject to salt screening, whereas most of the histone charges are buried inside nucleosomes and don't get screened. We chose partial charges in such a way that the nucleosomes remain 'slightly' negatively charged, which is consistent with electrophoresis experiments [S6]. The centers of charges considered in our calculations are: Cz, Nz in Arginine and Lysine with corresponding partial charge +1; Cd, Cg in Glutamate and Aspartate with partial charge –1, and the P atoms in nucleosomal DNA with partial charge –0.3. This level of neutralization is predicted in numerical computations [S7].

The long and flexible tails of H3 histones are cut away in our model, but their effect has been taken into account implicitly. According to the "coarse grained" MC simulations [30] the positively charged H3 tails are likely to align along the linkers, resulting in a significant neutralization of linker DNA. Therefore, the linker DNA was modeled with the partial charges –0.25 per nucleotide. (In addition, we varied these charges from –0.05 to –0.5; see section D.)

(III) Steric clashes. Steric clashes are modeled by a van der Waals-like repulsion potential. All the centers of charges considered above are included here, as well as the centers of the DNA base pairs. This is necessary because the P-P distances are relatively large when measured across the major groove, and it might happen that the nucleosomal DNA and the linkers penetrate if the base pairs are not considered. The van der Waals radii are assumed to be 3.0 Å for the centers of charges and 8.0 Å for the DNA base pair centers. The repulsion potential is calculated as

$$E_{vdW} = 10.0 \times \sum_{ij} \left(\frac{\sigma_i + \sigma_j}{r_{ij}}\right)^{12}$$

where σ_i , σ_j are the van der Waals radii, and r_{ij} is the distance between the corresponding pseudo-atoms.

(IV) H4 tail – acidic patch interactions.

Our model of the H4 tail – acidic patch interactions is based on three assumptions:

(i) To stabilize the inter-nucleosome stacking, the positively charged Lys16 (H4) of one nucleosome has to be in the immediate vicinity of the 'acidic patch center' of adjacent nucleosome [S8].

(ii) The acidic patch center coincides with Cd atom of Glu61 (H2A).

(iii) The flexible H4 tail can rotate freely around the hinge located at Asp24 (H4). This is based on comparison of H4 conformations in five crystal structures (Table S1 and Figure S1). In particular, the

distance between Asp24 (the presumed location of the hinge on H4 tail) and Lys16 (H4) varies from ~10 to ~35 Å. (In these calculations, the residues Asp24 and Lys16 were represented by their Ca and Nz atoms, respectively.)

Table S1. List of PDB structures used to calculate the Asp24 (H4) – Lys16 (H4) distances

PDB ID	Minimal distance (Å)	Maximal distance (Å)
T1- 1KX5	11	32
T2- 1AOI	19	24
T3- 1ZBB	20	29
T4- 3UT9	24	29
T5- 4KUD	19	27

References:

[T1] Davey, C.A., Sargent, D.F., Luger, K., Maeder, A.W., Richmond, T.J. (2002) *J. Mol. Biol.* **319:** 1097-1113

[T2] Luger, K., Mader, A.W., Richmond, R.K., Sargent, D.F., Richmond, T.J. (1997) *Nature* **389:** 251-260

[T3] Schalch, T., Duda, S., Sargent, D.F., Richmond, T.J. (2005) *Nature* **436:** 138-141

[T4] Chua, E.Y.D., Vasudevan, D., Davey, G.E., Wu, B., Davey, C.A. (2012) *Nucl. Acids Res*. **40:** 6338-6352

[T5] Yang, D., Fang, Q., Wang, M., Ren, R., Wang, H., He, M., Sun, Y., Yang, N., Xu, R.M. (2013) *Nat. Struct. Mol. Biol.* **20**: 1116-1118

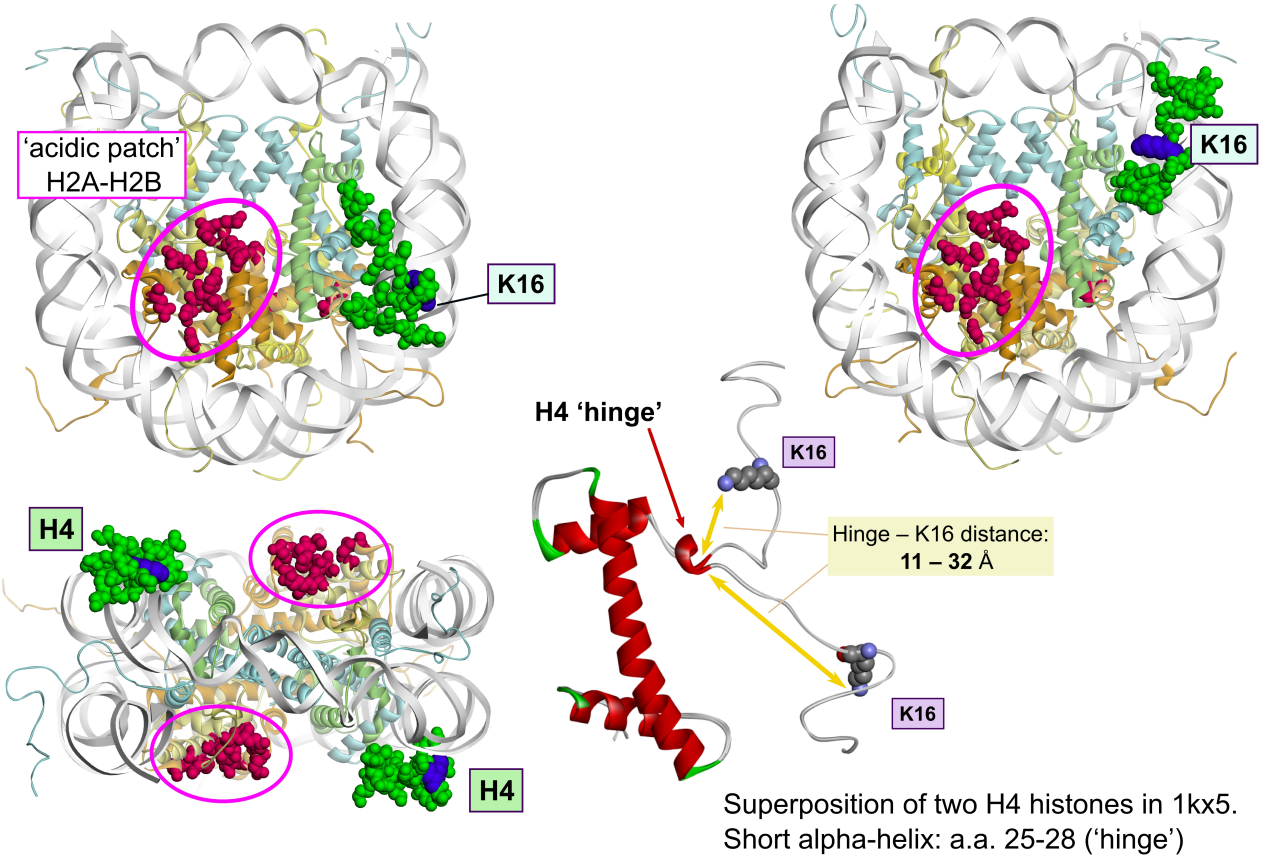

Figure S1. Two conformations of the H4 tail in nucleosome 1kx5.

The top view (left) and the bottom view (right) demonstrate different conformations of the H4 histone N-tail, in green (chains B and F, respectively). The acidic patches (histones H2A-H2B, red CPK atoms) are indicated by pink ellipses.

Center: Superposition of the two H4 chains shows a significant difference between the two N-tail conformations. At the same time, the short α-helix (residues 25-28) retains practically the same conformation in both H4 chains. Therefore, we assume that the N-tail can rotate freely around the 'hinge' located at the N-end of this α-helix, namely, at Asp24 (H4). Note that the distance between the positively charged Lys16 (atom Nz) and the hinge at Asp24 (atom Ca) varies from 11 to 32 Å in the two conformations of histone H4.

Bottom left: The side view of nucleosome 1kx5 [1], with the H4 histone N-tails and acidic patches indicated.

The attractive interactions between the H4 tail and the acidic patch are modeled phenomenologically. We calculate the distance x between the hinge, Asp24 (H4), and the patch center, Glu61 (H2A), located on two adjacent nucleosomes. The energy of the tail-patch interaction as a function of the distance x is approximated by the flat-well potential:

$$E_{tail-patch} = C \times \left(\frac{x-d_2}{1+|x-d_2|} + \frac{d_1-x}{1+|d_1-x|} \right)$$

where C = 4.35 kT defines the depth of the potential and d_1 = 10 Å and d_2 = 35 Å are the positions of two walls of the well (Figure S2). The energy calculated in this way corresponds to formation of two 'bridges' between two stacked nucleosomes (Figure S3). Note that in addition to the electrostatic attraction between the basic H4 tails and the acidic patches on H2A/H2B histones, this potential implicitly includes the van der Waals and hydrophobic interactions stabilizing the inter-nucleosome stacking. The depth of the potential, –8 kT, was selected as an intermediate between two experimentally measured values for the inter-nucleosome stacking, –3.4 kT [49] and –13.8 kT [8]. In addition, we made computations with the stacking energy –5 kT, and found that the main results (such as the positions of the total energy minima shown in Figure 3) remain practically the same. Figure S4 shows how the total energy varies by the changes in the depth of the stacking potential.

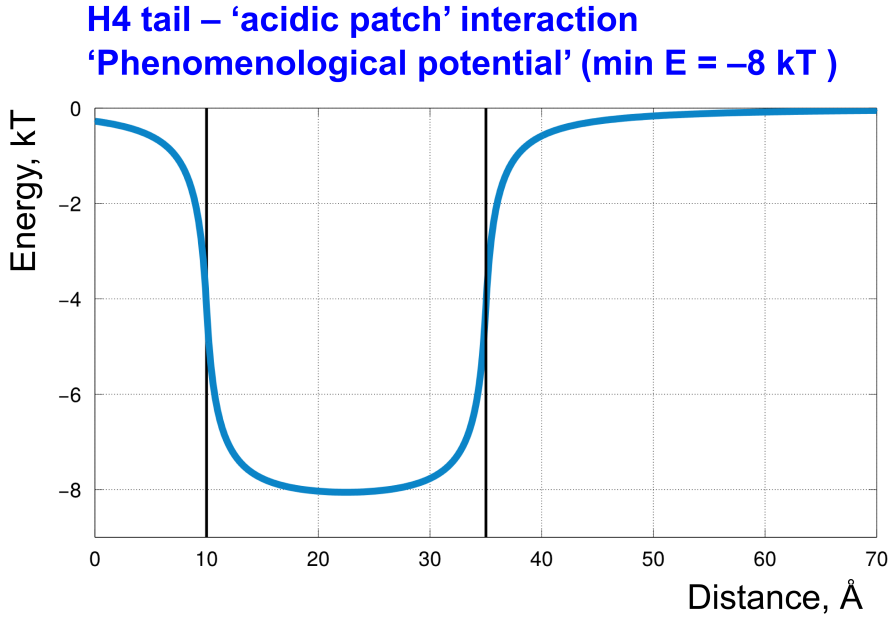

Figure S2. Phenomenological potential describing the H4 tail – acidic patch interactions.
Note that the interval between two walls of this flat-well potential, d_1 = 10 Å and d_2 = 35 Å, covers the minimal and maximal distances Asp24 (H4) – Lys16 (H4) presented in Table S1.

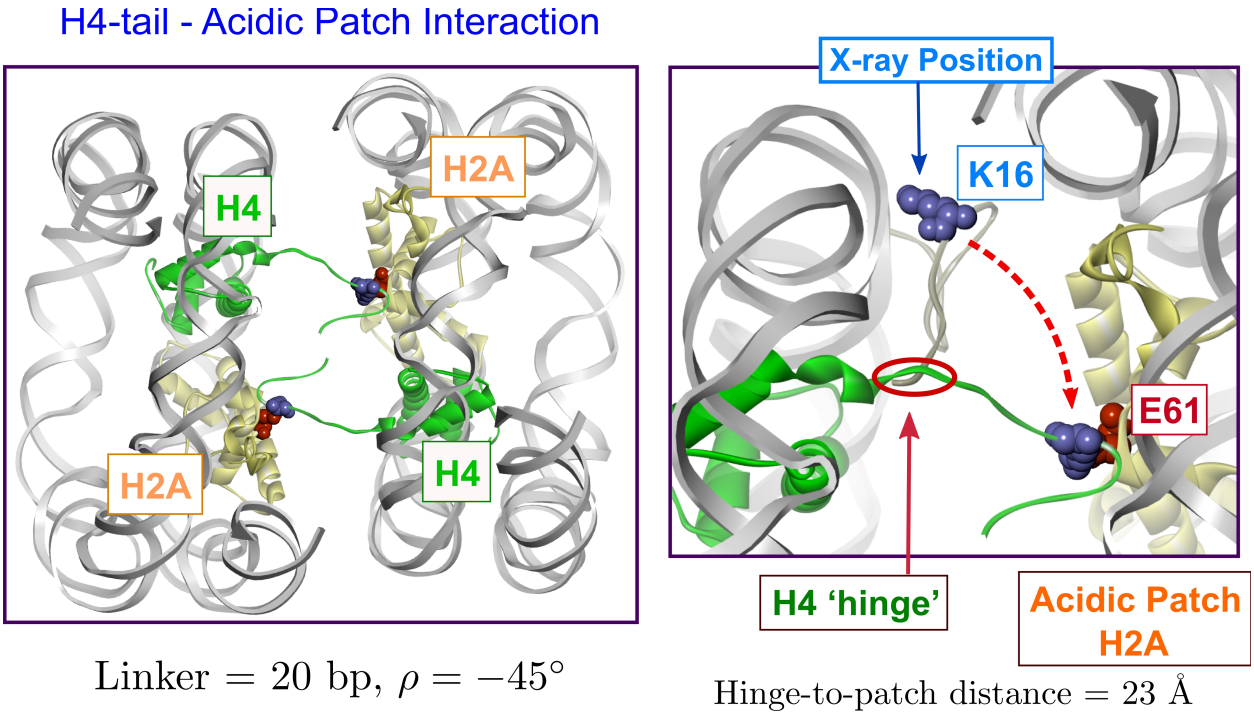

Figure S3. Visualization of the H4 tail – acidic patch 'bridges.'

Left: Two H4 – H2A 'bridges' stabilize the inter-nucleosome stacking. The optimal configuration of the nucleosome fiber with linker L=20 bp is shown, with the inclination angle $\rho = -45°$.

Right: The H4 tail rotates around the 'hinge' to bring the positively charged Lys16 (H4) in the close vicinity of the 'acidic patch' of adjacent nucleosomes. In this particular structure, the distance between the 'hinge' at Asp24 (H4) and the patch center at Glu61 (H2A) is 23 Å. Note that this distance corresponds to the minimum of the potential presented in Figure S2.

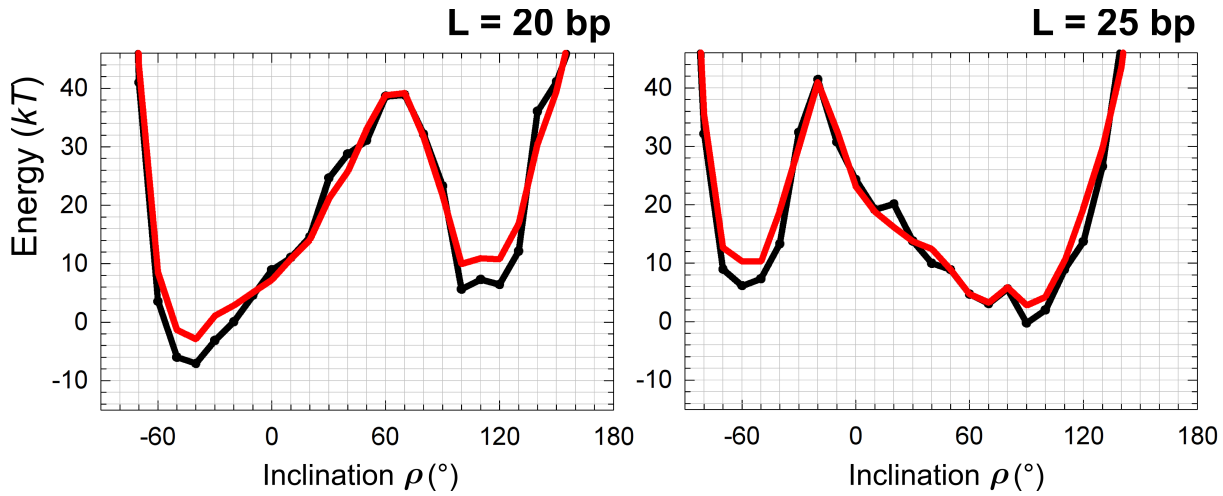

Figure S4. Total energy profiles for two H4 tail – acidic patch interaction potentials.

The black curves correspond to stacking energy –8 *kT* used in the main text (compare with Figure 3). Changing this value to –5 *kT* (red curves) increases the energy values in local minima. Note that positions of the minimal points and general form of energy profiles do not change.

C: Total energy minimization

The energy terms described above are calculated per fiber asymmetric unit, consisting of the nucleosome core and the 'downstream' linker (Fig. 1A). The energy of interaction between units #i and #j is denoted by E(i,j), and the internal energy of unit #i is denoted by E(i). Then, the total energy per unit can be written as E_{total} = E(i) + E(i,i+1) + E(i,i+2). The interactions with units #i+3, #i+4, etc. are ignored due to the distance cutoffs. Interactions with the 'preceding' nucleosomes are not considered due to the symmetry and regularity of the fiber. For example, interaction E(i-1,i) is equivalent to E(i,i+1) and it is assigned to the unit #i-1.

During minimization of the total energy, for each selected set of the four superhelical parameters (Fig. 1), the linker DNA is optimized as described above. The DNA elastic energy is calculated during this cycle of minimization. Another, outer cycle of minimization, is used to optimize the total energy of the fiber. To make sure that the optimized conformations are not just randomly selected local minima, ~300,000 points in the 4D space of fiber parameters were considered as starting points.

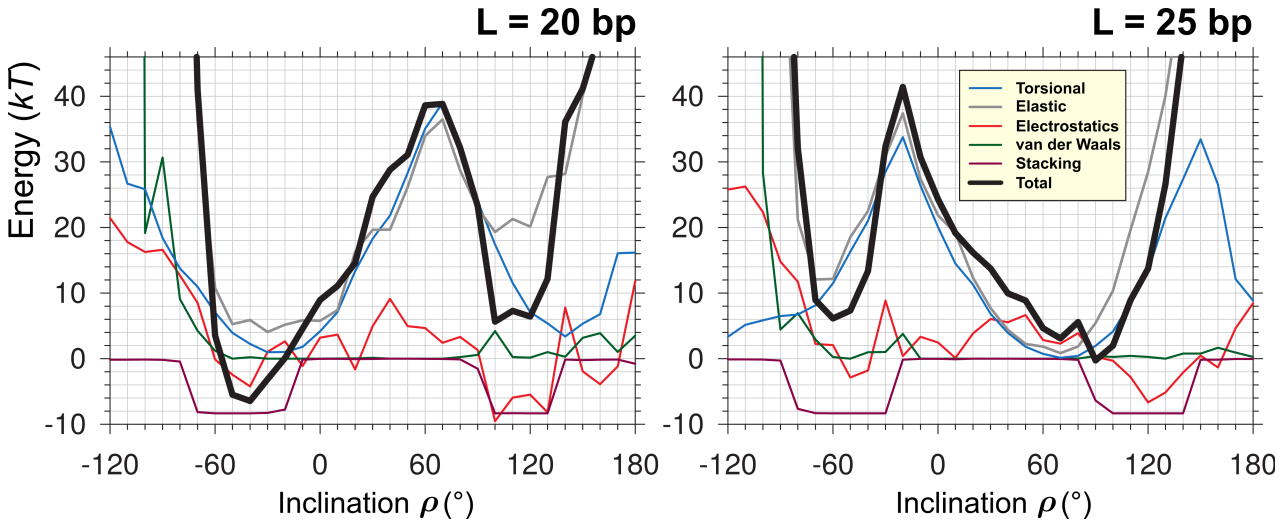

Figure S5. Total fiber energy as a function of inclination angle ρ. Optimization is made in the space of three remaining fiber parameters, i.e. radius, rise, and polar angle φ (Fig. 1). All energy terms are shown separately. The torsional energy profiles (blue curves) have two approximately equal minima separated by topological barriers. Adding other energy terms changes the minima depths and positions, but bimodality of the energy profiles remains.

For example, adding the van der Waals (green) and electrostatic (red) energy terms makes the structures with $\rho < -90°$ and $\rho > 130°$ extremely unfavorable. Furthermore, electrostatic interactions are repulsive for the inclination angle in the interval $30° < \rho < 60°$, therefore, the 'right' minimum for L=25 bp is shifted to $\rho = 90°$ (compared to the torsional energy minimum at $\rho = 70°$). Finally, the regions of optimal stacking interactions (purple curves) are nearly the same for both L=20 and 25 bp, $-70° < \rho < -30°$ and $90° < \rho < 130°$.

D: Electrostatic Interactions

We used two ways to account for the electrostatic interactions in the nucleosome fibers. One approach (presented in the main text) is using Coulomb potential with distance cutoff 30 Å, along with the charge reduction due to the counterion screening. The second approach is using Debye-Huckel potential with the (in vitro) Debye length 8.3 Å [31]. Comparison between energy profiles obtained by the two methods is shown in Figure S6. Importantly, we found that changing the details of electrostatic potential does not change qualitatively the total energy profiles.

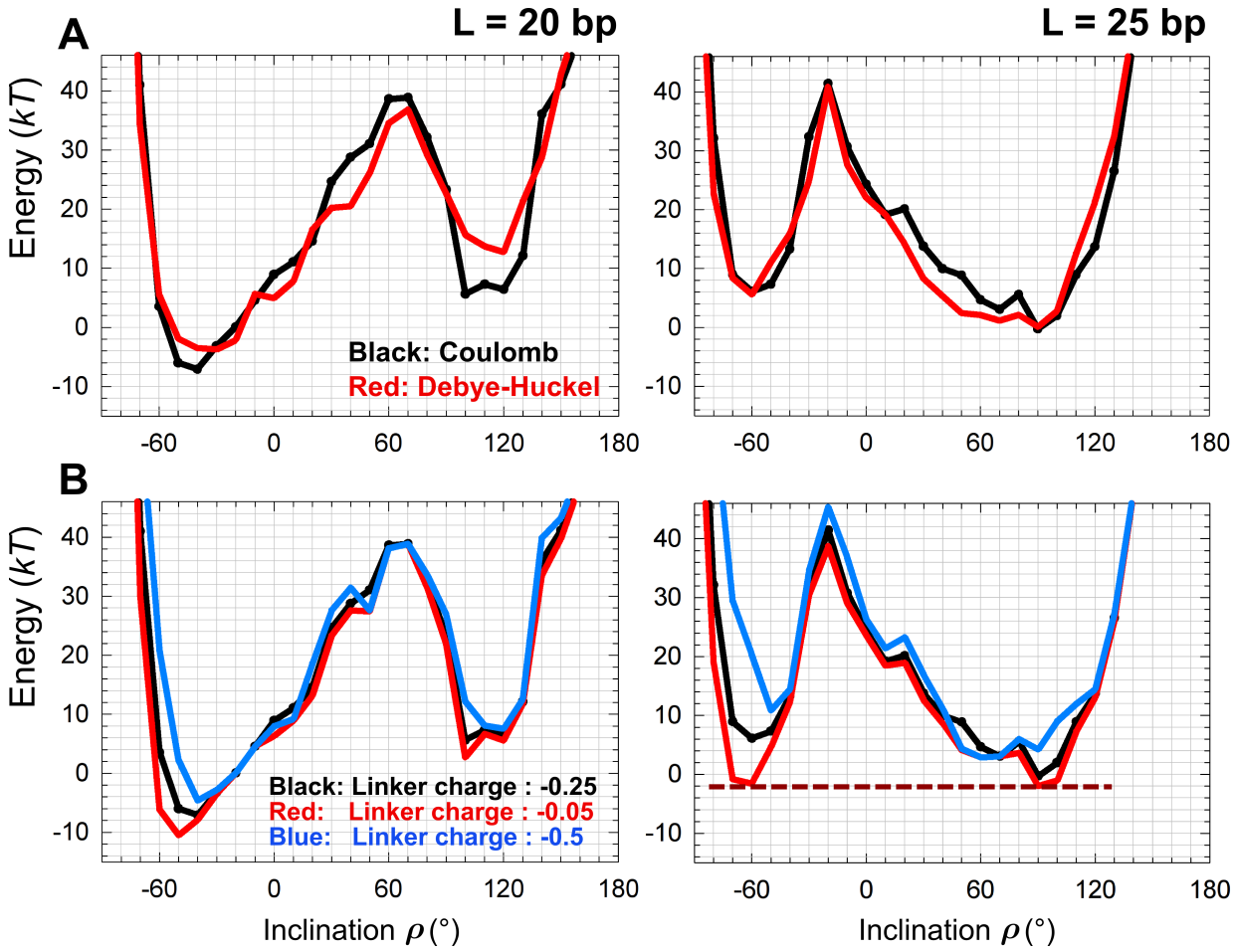

Figure S6. Dependence of the total energy profiles on electrostatic potential.

(A) Black curves correspond to Coulomb potential and red curves correspond to Debye-Huckel potential. Charge on the linker DNA is –0.25 per phosphate (as in the main text).

(B) Effect of the linker DNA charges on the relative stability of the fiber topoisomers (Coulomb potential). Black curves reproduce the main text results, for the linker DNA charge –0.25 per phosphate, blue curves are for the charge –0.5 per phosphate (weak DNA neutralization), and red curves are for the charge –0.05. In the latter case the linker DNA neutralization is the strongest; it may be caused, for example, by linker histones or histone H3 tails (Figure S8). Note that the energy profile is more affected for L=25 than for L=20 bp. In particular, when the charge density is the smallest, –0.05, the left minimum at $\rho = -60°$ becomes as deep at the right one at $\rho = 90°$ (L=25 bp). Figure S7 shows why electrostatic effects are more pronounced in the T2 structures with $\rho < 0$.

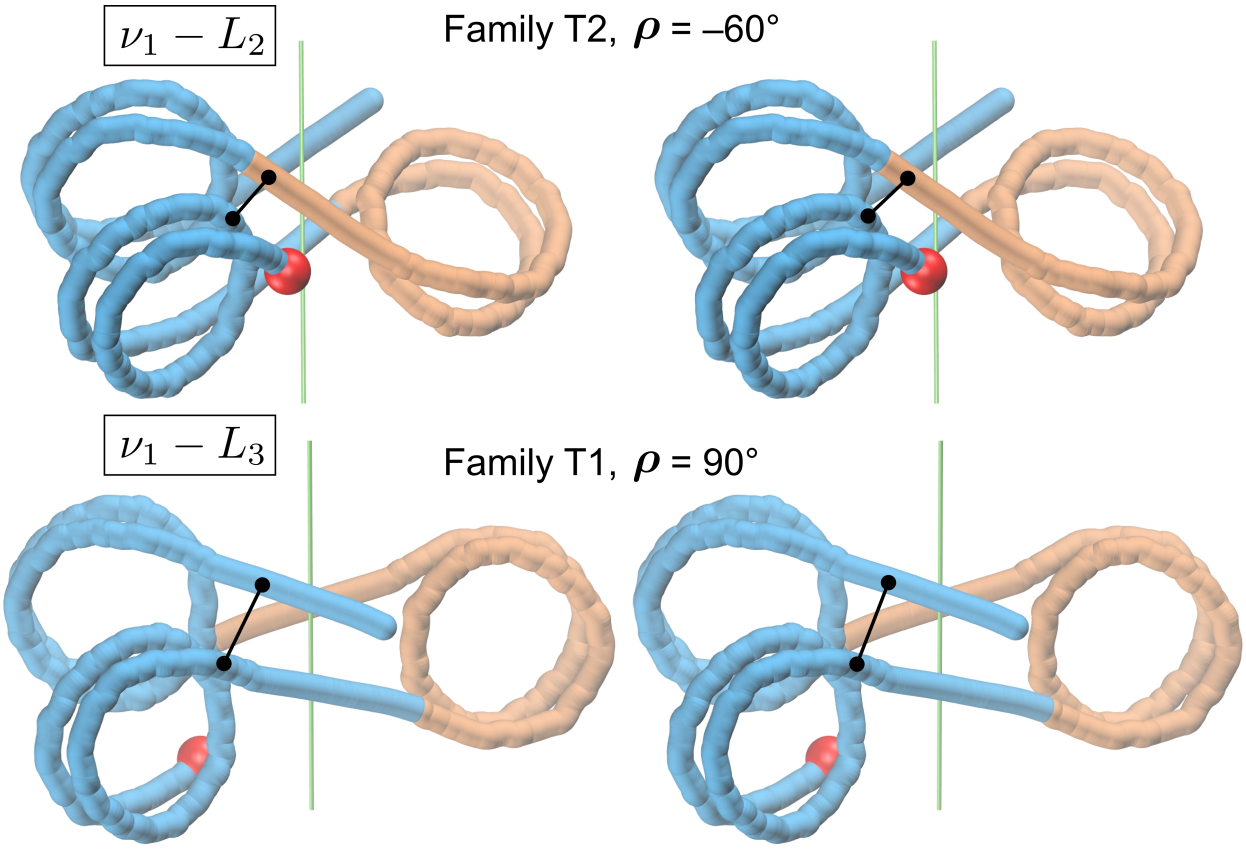

Figure S7. Electrostatic DNA-DNA interactions in the optimal fiber structures with L=25 bp. The T2 (top) and T1 (bottom) conformations are presented in stereo. The closest distances between the core and linker DNA are shown by black segments: in the T2 structure, the distance is between the ν1 core DNA and the linker L2, while in the T1, it is between ν1 and L3. The distances for the T2 structure are shorter than for the T1 (~30 and ~40 Å, respectively); therefore electrostatic repulsion is stronger in T2. This difference explains the result presented in Figure S6B – the decrease in the DNA charge density deepens the left energy minimum (family T2, $\rho < 0$) more than the right minimum (family T1, $\rho > 0$; L=25 bp). The larger DNA-DNA distances in the T1 conformations would make the linker DNA more accessible for various transcription factors. The red balls denote entry points of ν1, see Figure 1. The green vertical lines indicate the fiber axes.

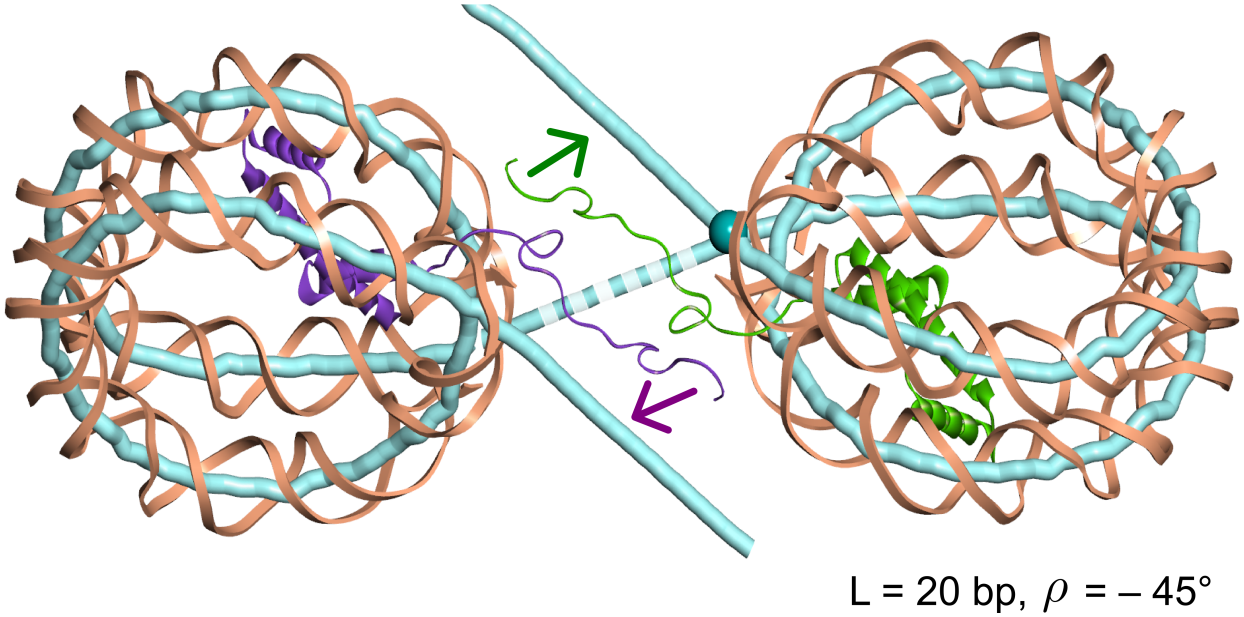

Figure S8. H3 tail – linker DNA interaction.

Mutual orientation of the shown nucleosomes corresponds to the optimal fiber conformation for L=20 bp (compare with Figure S9). In both nucleosomes, the histone H3 is represented by the chain A in the 1kx5 structure [1]. In this conformation, the H3 tail 'covers' 10-15 bp fragment of linker DNA. Our model is consistent with that proposed by Perisic et al. [30] based on Monte Carlo simulations. In yeast, where the linker histone is strongly underrepresented compared to the core histones [S9,S10], the shown scheme is likely to be one of the main mechanisms of the linker DNA neutralization.

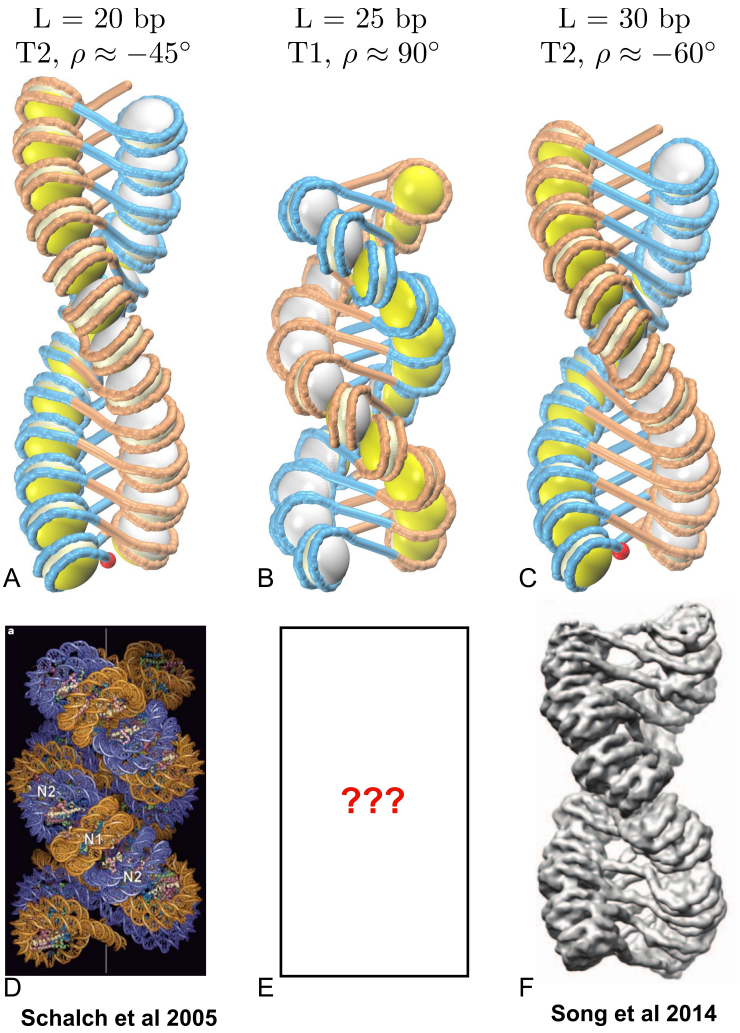

Figure S9. Comparison with the experiment-based models.

Our optimal structures for L = 20, 25, and 30 bp are shown in the first row. In the second row the published experiment-based models are given for comparison. For L=20 bp, our optimal structure has inclination angle –45° and rise = 27 Å (Figure 8). The 'direct' model by Schalch *et al.* [10] is based on the X-ray tetranucleosome structure; it has an inclination angle about –50°/–40° and rather low rise = 17 Å. Note, however, that this model has "steric overlaps" [10]; the authors suggest that these overlaps can be "relieved by increasing the separation of "tetranucleosomes." On the other hand, using the EM images for the '601' nucleosome arrays with NRL=167 [7,12], one can estimate the rise value as 25 Å, which is close to our evaluation of rise = 27 Å. For L=30 bp, Song et al. [11] built their model based on the Cryo-EM data, with the inclination angle –60° and rise = 24 Å. Our optimal structure is very close to this model: $\rho \approx -60°$ and rise = 25 Å. For L=25 bp, our optimal structure has $\rho = 90°$ and rise = 23 Å. Note that there are no experiment-based models for L=25 bp.

E: Symmetrization of the nucleosome structure

To make sure that our results are consistent with the requirement of symmetry of a nucleosome fiber, we used the symmetrized version of the 1kx5 structure [1]. To this aim, the chains E, F, G and H were replaced by the superimposed copies of the chains A, B, C and D (histones H3, H4, H2A and H2B respectively). The symmetrization procedure was made using MatchMaker tool of Chimera [S11].

F: Computation of DNA writhing and linking number

To evaluate the topological changes occurring in DNA upon formation of a nucleosome fiber, we are using the three topological parameters: ΔTw (the change in DNA twisting), DNA writhing, Wr, and the change in the linking number, ΔLk (compared to the relaxed state of DNA), which are related by well-known equation: $\Delta Lk = \Delta Tw + Wr$ [34-38]. This equation is valid for the closed circular DNA, therefore, we need to find an effective way to calculate Wr of DNA packaged in a nucleosome fiber, so that the result does not depend on selection of the closed DNA trajectory.

To calculate the DNA Writhing we use the quadrangle approach described by Levitt [37] and Klenin and Langowski [38]. The DNA trajectory is described as a polygonal chain with the vertex points at the centers of base pairs. The DNA twisting is determined using the Euler angle formalism [S12] implemented in CompDNA [S13] and 3DNA [S14] software. (*– see below.) After generating the fiber as described in the main text we added 25 or 200 extra points connecting the ends of DNA in a way that the closing chain does not pass through nucleosomes (Figure S10). We found that the open 10-nucleosome trajectories and the closed ones (with 25 extra points) produce different average Wr values, varying by as much as 0.23 per nucleosome (Table S2). On the other hand, the open and the closed 100-nucleosome trajectories produce very close Wr values, with the difference not exceeding 0.05. In the case of 200 extra points (connecting the ends of DNA) this difference does not exceed 0.03.

Therefore, we conclude that calculating the DNA writhing for the open 100-nucleosome fibers is an adequate way to estimate the topological changes in DNA upon formation of a nucleosome fiber.

(*) The DNA twisting is computed only for the linkers. Twisting of the nucleosomal DNA may be somewhat different from that of free DNA [S15], but this difference is not essential for our purpose, because it remains the same for different fiber structures, as long as the nucleosome cores retain the same conformation.

Table S2

DNA Writhing per nucleosome

Linker (bp)	Angle ρ	10 nsm open	10 nsm closed *	$\delta(Wr)$ 10 nms	100 nsm open	100 nsm closed *	$\delta(Wr)$ 100 nsm	100 nsm closed, 200 points added
20	-70	-1.57	-1.69	0.12	-1.67	-1.71	0.03	-1.69
20	-40	-1.35	-1.58	**0.23**	-1.50	-1.55	**0.05**	-1.53
20	40	-1.09	-1.10	0.01	-1.13	-1.09	0.04	-1.10
20	70	-0.99	-0.92	0.07	-1.00	-0.98	0.02	-1.00
25	-70	-1.57	-1.69	0.12	-1.67	-1.70	0.03	-1.69
25	-40	-1.39	-1.57	0.17	-1.52	-1.55	0.03	-1.52
25	40	-1.09	-1.11	0.02	-1.12	-1.12	0.01	-1.12
25	70	-0.96	-0.92	0.05	-1.00	-0.98	0.02	-0.99

* 25 points added, connecting the ends of DNA in nucleosome fiber (Figure S10).
$\delta(Wr)$ is the difference between the two *Wr* values obtained for the open and closed nucleosome fiber.
The largest values are in boldface underlined.

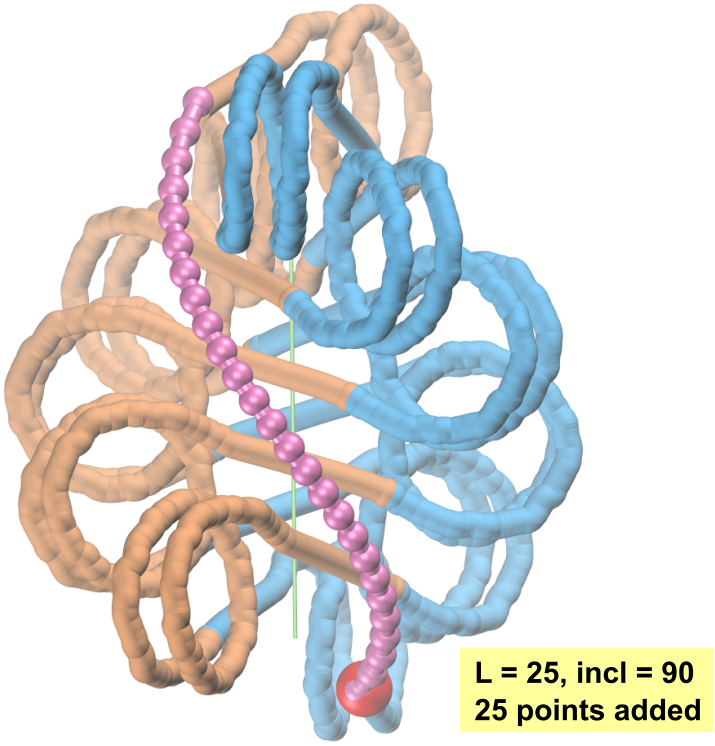

Figure S10. Illustration of the DNA chain closure, used to calculate DNA writhing in the nucleosome fiber. 25 extra points are added (shown in pink) to make the closed DNA trajectory.

G: Movie. Fiber conformation as a function of the inclination angle

The movie "30-nm-Rho-Variation" visualizes changes in the two-start fiber conformation caused by a gradual increase in the inclination angle ρ from –180° to 180° (linker L=20 bp). The increase in inclination angle is accompanied by the clock-wise rotation of the red ball at the bottom, denoting the DNA 'entry point.' Notice over-crossing of the linkers at $\rho \approx -120°$ (shown by ellipses). All the shown structures are optimal for the given inclination (Figure 3A). There are two versions of the movie -- one is for PC users (with extension .avi) and the other is for MAC users (with extension .mov).

H: Right-handed two-start fibers

Small angle X-ray scattering analysis of the nucleosome fibers performed by Williams et al. [13] suggests formation of the left-handed two-start superhelices in solution. The X-ray crystallography and Cryo-EM imaging also support the left-handed organization of two-start fibers [10-11]. To check if our model is consistent with these results, we analyzed the right-handed fibers using the same minimization procedure (described in the main text). To this aim, we assumed that the polar angle φ varies between 180° and 210° (Figure 1). (Note that for the left-handed two-start fibers the angle φ varies between 150° and 180°.)

We found that the optimal energy for the right-handed helices is significantly higher than for the left-handed ones (Figure S11). This energy difference is more pronounced for L=25 bp (~12 kT) than for L=20 bp (~6 kT). As follows from the comparison of the two types of fibers, the linker-nucleosome clashes prevent formation of a strong stacking between nucleosomes in the right-handed superhelices. In summary, we conclude that the chirality of nucleosomes dictates the left-handedness of the chromatin fiber.

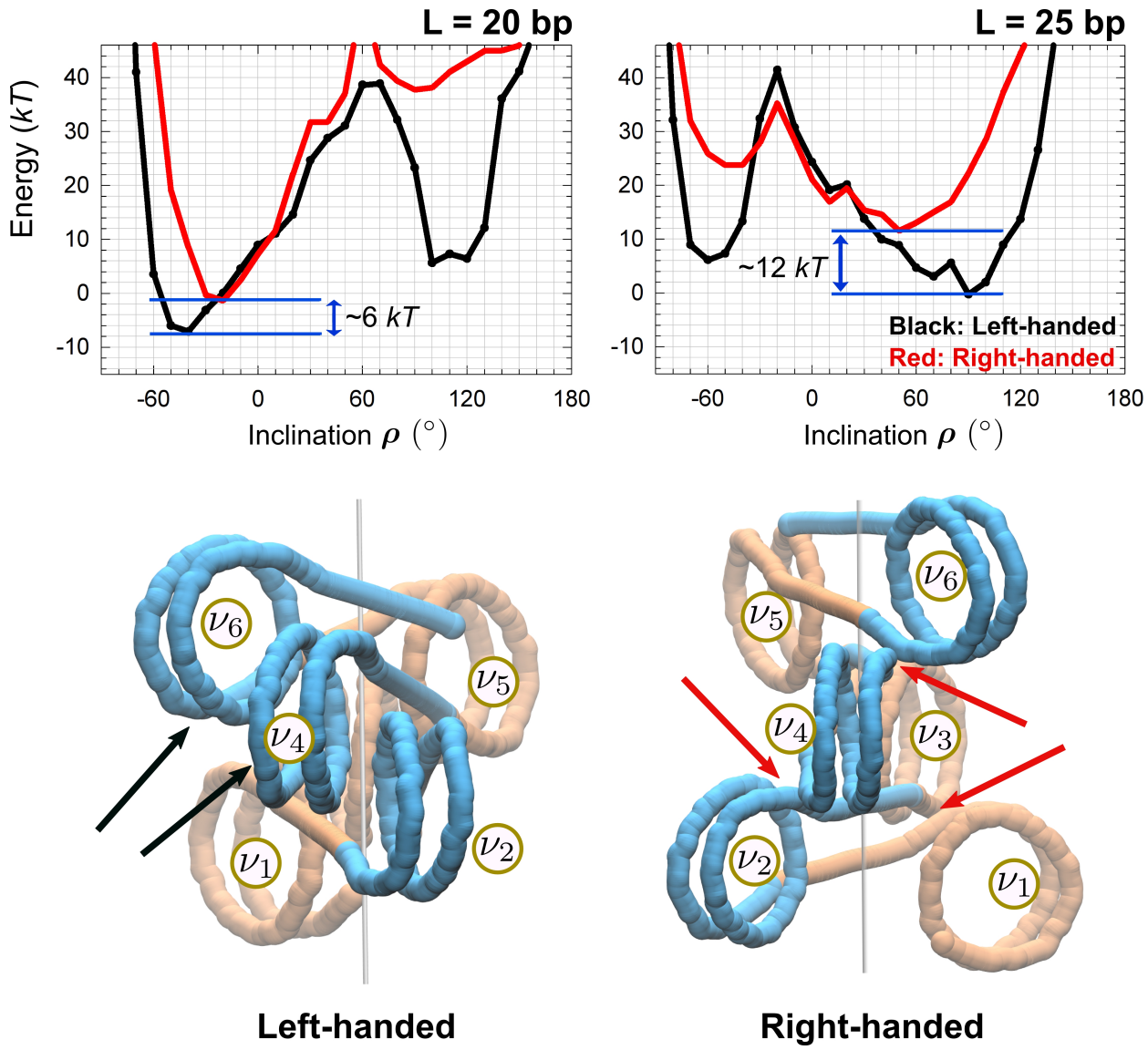

Figure S11. Comparison between the left-handed and right-handed nucleosome fibers.

Top. Total energy profiles for the left-handed (black curves) and right-handed (red curves) fibers. The minimal energy is higher in the right-handed structures, mostly due to electrostatic repulsion between the core DNA and the linkers (shown in the bottom). Note that the right minimum (at $\rho \approx 90°$) is influenced more by change in the fiber handedness.

Bottom. Optimal structures with $\rho = 90°$, L = 25 bp are shown. The left-handed fiber is tightly packed with a strong inter-nucleosome stacking (black arrows) while the right-handed fiber needs a large rise to avoid clashes (close contacts shown by red arrows); as a result, the stacking is disrupted. The nucleosomes are numbered to clarify their connectivity in fibers.

I: Linking number in chromatin fibers with various linker lengths

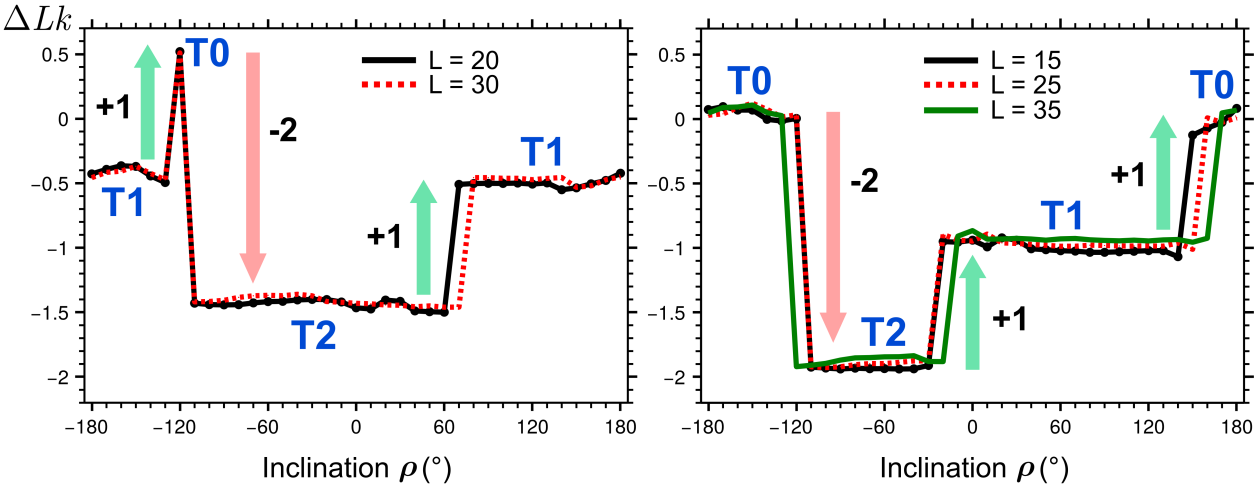

Figure S12: Linking number per nucleosome as a function of inclination angle ρ for selected linker lengths, L. *Left:* the data for L = 10n (20 and 30 bp); *right:* the data for L = 10n+5 (15, 25, and 35 bp). The linking number is (almost) piecewise constant in the three regions corresponding to the three topological families, T2, T1 and T0 (see Figure 7D). The T2 family consists of the fiber conformations with the lowest ΔLk values (from approximately −2.2 to −1.5). The fibers with intermediate ΔLk (from −1.2 to −0.5) comprise family T1. The family T0 corresponds to the highest ΔLk values (from approximately 0 to 0.5). Note that for L = 20 and 30 bp, the T0 family is represented by a single point $\rho = -120°$ (in this particular presentation with the ρ increment of 10°).

The inter-family transitions are accompanied by abrupt changes in ΔLk values shown by red arrows (decrease in ΔLk) and green arrows (increase in ΔLk). The sharp transition between the families T0 and T2 (red arrows) is accompanied by $\Delta(\Delta Lk) \approx -2$ and occurs around $\rho = -120°$ for all linkers. By contrast, the T2-T1 and T1-T0 transitions occur at different ρ values depending on the linker length, L; these transitions are accompanied by $\Delta(\Delta Lk) \approx +1$. The structural nature of these transitions is discussed in the Results section, see Figure 7.

Using the ΔLk values, we can calculate the superhelical density of DNA, σ, defined as (number of superhelical turns) divided by (number of turns of DNA in relaxed state, N_r). Normalizing both values per one nucleosome, we have $\sigma = \Delta Lk / N_r = \Delta Lk /$ (NRL/10.45), where NRL is nucleosome repeat length, and 10.45 is the average number of DNA base pairs per turn.

The energetically optimal fibers are characterized by the values:

L = 20 bp, NRL =167 bp, $\Delta Lk = -1.5$ (Figures 7C, D), $\sigma = -0.09$
L = 25 bp, NRL =172 bp, $\Delta Lk = -1.0$ (Figures 7C, D), $\sigma = -0.06$

Note that these values of σ are consistent with the experimental measurements for both pro- and eukaryotes [47]; in particular, $\sigma \approx$ -0.06 for *E. coli*. In other words, the torsional stress experienced by DNA if the histones are removed, is comparable with the torsional stress in bacteria.

Supplementary References

S1. Go, N. & Scheraga, H.A. Ring Closure and Local Conformational Deformations of Chain Molecules. *Macromolecules* 1970, 3:178-187.

S2. Zhurkin, V.B., Lysov, Y.P. & Ivanov, V.I. Different families of double-stranded conformations of DNA as revealed by computer calculations. *Biopolymers*. 1978, 17:377-412.

S3. Olson, W. K., Marky, N. L., Jernigan, R. L. & Zhurkin, V. B. Influence of fluctuations on DNA curvature. A comparison of flexible and static wedge models of intrinsically bent DNA. *J. Mol. Biol*. 1993. 232: 530-554.

S4. Dickerson, R. E., Bansal, M., Calladine, C. R., Diekmann, S., Hunter, W. N., Kennard, O. Lavery, R., Nelson, H. C. M., Olson, W. K., Saenger, W., Shakked, Z., Sklenar, H., Soumpasis, D. M., Tung, C -S., Kitzing, E. V., Wang, A. H. -J. & Zhurkin, V. B. Definitions and nomenclature of nucleic acid structure parameters. *EMBO J*. 1989. 8: 1-4.

S5. Kosikov, K.M., Gorin, A.A., Zhurkin, V.B. & Olson, W.K. DNA stretching and compression: large-scale simulations of double helical structures. *J Mol Biol*. 1999, 289:1301- 1326.

S6. Hewish, D.R. & Burgoyne, L.A. Chromatin sub-structure. The digestion of chromatin DNA at regularly spaced sites by a nuclear deoxyribonuclease. *Biochem Biophys Res Commun*. 1973, 52:504-510.

S7. Materese, C.K., Savelyev, A. & Papoian, G.A. Counterion atmosphere and hydration patterns near a nucleosome core particle. *J Am Chem Soc*. 2009, 131:15005-15013.

S8. Yang, D. & Arya, G. Structure and binding of the H4 histone tail and the effects of lysine 16 acetylation. *Phys Chem Chem Phys*. 2011, 13:2911-2921.

S9. Freidkin, I. & Katcoff, D.J. Specific distribution of the Saccharomyces cerevisiae linker histone homolog HHO1p in the chromatin. *Nucleic Acids Res*. 2001, 29, 4043–4051.

S10. Downs, J.A., Kosmidou, E., Morgan, A. & Jackson, S.P. Suppression of homologous recombination by the Saccharomyces cerevisiae linker histone. *Mol. Cell* 2003, 11, 1685–1692

S11. Pettersen, E.F., Goddard, T.D., Huang, C.C., Couch, G.S., Greenblatt, D.M., Meng, E.C. & Ferrin, T.E. UCSF Chimera -- a visualization system for exploratory research and analysis. *J Comput Chem*. 2004, 25:1605-1612.

S12. Zhurkin, V.B., Lysov, Y.P., & Ivanov, V.I. Anisotropic flexibility of DNA and the nucleosomal structure. *Nucleic Acids Res*. 1979. 6:1081-1096.

S13. Gorin, A. A., Zhurkin, V. B., & Olson, W. K. B-DNA twisting correlates with base pair morphology. *J. Mol. Biol*. 1995, 247: 34-48.

S14. Lu, X. & Olson, W.K. 3DNA: a versatile, integrated software system for the analysis, rebuilding and visualization of three-dimensional nucleic-acid structures. *Nat Protoc* 2008, 3:1213-1227.

S15. Richmond, T.J. & C.A. Davey, The structure of DNA in the nucleosome core. *Nature*, 2003. 423(6936): p. 145-50.